Formation Control for Quad-Rotor Aircrafts Based on Potential Functions

Luis Arturo García Delgado and Alejandro Enrique Dzul López*
Instituto Tecnológico de la Laguna
Blvd. Revolución y Czda. Cuauhtémoc S/N CP 27000, Torreón, Coah., México
* dzul@faraday.itlalaguna.edu.mx
Teléfono: (871) 705-13-13.

***Abstract*— This paper presents a decentralized formation control scheme for a group of quad-rotor rotorcrafts. The control scheme for the aircraft group is based on potential field theory while the control law for each rotorcraft is based on nested saturation. The potential function dictates the direction toward each rotorcraft is going to move, so that, the trajectories will be generated by this way, guaranteeing collision avoidance. The problem of obstacle avoidance is also presented, using a potential repulsive function.**

Palabras clave: Formation Control, Aircraft Control, Nonlinear Control Systems, Saturation Control.

I. INTRODUCTION

The works in literature about mobile robots have been changing from a single vehicle to a group of vehicles. The tasks in which more than one robot are involved with at least one target in common, receive the name of *cooperation*. One field of cooperative control is the vehicles formation.

The vehicles formation has been widely studied for wheeled mobile robots (WMR's), airplanes, and with particles, however, in literature we barely find papers that deals about helicopters' formations (M. Saffarian and F. Fahimi, 2007), (M. Saffarian and F. Fahimi, 2008), (T. Paul et al., 2008), (F. Fahimi, 2008), since their nonlinear under-actuated dynamics and high coupling effects among vehicles states variables. Compared to other aerial vehicles, helicopters possess considerable maneuvering capabilities, which make them attractive to be considered for many applications (M. Saffarian and F. Fahimi, 2007).

A way to deal with the formation problem is through a leader-follower structure, in which each vehicle follows another vehicle. This kind of structure is hierarchical, and there is not enough relation among every vehicle in the formation, just between leader and follower. If the position error is no zero between a leader and a follower, and the follower is leader of other vehicles as well, the error between the main leader and the farthermost follower, in the formation structure, could be even bigger. Also, one characteristic in the leader-follower structure is the next: if an object obstructs the way of a vehicle in the formation path, while this vehicle tries to avoid the obstacle, the other vehicles follow their normal path and the formation is lost until the obstacle has been avoided (T. Dierks and S. Jagannathan, 2009). A possible disadvantage in the leader-follower structure is that the formation control depends on the dynamical model of the vehicle, and if there exist parametric uncertainties, then an adaptive control law is designed, by which the control term becomes more complicated. However, a great advantage in this scheme is a fast response to reach the formation, and a tracking control may reduce the formation errors during movement.

Other way to reach a multi-vehicle formation is through potential field method. The basic concept of the potential field method is to fill the robot workspace with an artificial potential field in which the robot is attracted to its goal position and is repulsed away from the obstacles. This method is particularly attractive because of its mathematical elegance and simplicity (S. S. Ge and Y. J. Cui, 2000). It consists in generate artificial functions that attract or repulse the rotorcrafts to the point of minimal potential energy. We can find this kind of scheme in literature to stabilize a formation of WMR's (Yi Liang and Ho-Hoon Lee, 2006). The potential energy acts through a potential force that leads each rotorcraft to any position to construct the formation. The potential functions don't depend on the vehicle's model, they just give the forces vectors, and a particular control law will be responsible to move the vehicles according to the computed forces. In this paper we propose the way to link the computed potential force with a quad-rotor controller based on nested saturation (P. Castillo et al., 2005a).

This paper is organized as follows. In section II is described the dynamical model of the quad-rotor aircraft. Section III presents the formation control. In section IV some simulation results are presented, and in section V some conclusions are given.

II. DYNAMICAL MODEL

In this section is described the model of the quad-rotor aircraft, using a Lagrange approach. The generalized coordinates for the quad-rotor are the following

$$\boldsymbol{q} = (x, y, z, \phi, \theta, \psi) \in \mathbb{R}^6 \tag{1}$$

This work was supported by DGEST and CONACyT.

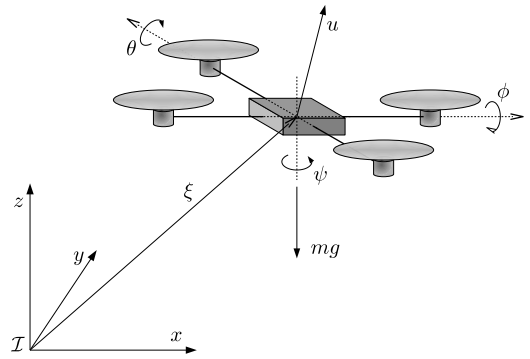

Fig. 1: Quad-rotor rotorcraft

where $\boldsymbol{\xi} = (x, y, z) \in \mathbb{R}^3$ denotes the position of the center of mass of the rotorcraft, relative to the inertial frame $\mathcal{I}$, and $\boldsymbol{\eta} = (\phi, \theta, \psi) \in \mathbb{R}^3$ represents the Euler angles that describe the rotorcraft orientation (see Figure 1).

The model used is the Euler-Lagrange approach used in (A. Sanchez et al., 2008)

$$\begin{aligned} m\ddot{x} &= u(\cos\psi\sin\theta\cos\phi + \sin\psi\sin\phi) && (2)\\ m\ddot{y} &= u(\sin\psi\sin\theta\cos\phi - \cos\psi\sin\phi) && (3)\\ m\ddot{z} &= u\cos\theta\cos\phi - mg && (4)\\ \ddot{\psi} &= \tau_\psi && (5)\\ \ddot{\theta} &= \tau_\theta && (6)\\ \ddot{\phi} &= \tau_\phi && (7) \end{aligned}$$

To simplify the model, through a controller, we are going to assume that $\psi = 0\ \forall t > 0$, thus

$$\begin{aligned} m\ddot{x} &= u\sin\theta\cos\phi && (8)\\ m\ddot{y} &= -u\sin\phi && (9)\\ m\ddot{z} &= u\cos\theta\cos\phi - mg && (10)\\ \ddot{\psi} &= \tau_\psi && (11)\\ \ddot{\theta} &= \tau_\theta && (12)\\ \ddot{\phi} &= \tau_\phi && (13) \end{aligned}$$

III. FORMATION CONTROL

III-A. Interactive Potential Energy

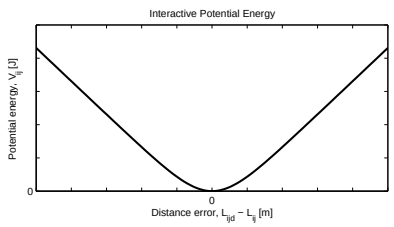

Fig. 2: Graph of the potential energy function

In this section we use an artificial potential function which is responsible to guide each rotorcraft to its position in the formation, avoiding collisions among them. Assume that the altitude z is maintained constant, such that the formation is going to be realized in a 2-D environment. With this assumption, the translational vector, expressing the position of the rotorcraft i is represented by

$$\boldsymbol{\xi}_i = \begin{bmatrix} x_i \\ y_i \end{bmatrix} \tag{14}$$

The distance between i^{th} and j^{th} rotorcrafts is

$$L_{ij} = \|\boldsymbol{\xi}_j - \boldsymbol{\xi}_i\| \tag{15}$$

and the formation distance error is represented by

$$\widetilde{L}_{ij} = L_{ijd} - L_{ij} \tag{16}$$

where L_{ijd} is the desired separation between the i^{th} and the j^{th} rotorcrafts. The artificial potential energy function chosen between the aircrafts i and j is a variation of the function used in (Yi Liang and Ho-Hoon Lee, 2006), and is

$$\mathcal{U}_{ij} = K_{ij} b_{ij}^2 \ln\left(\cosh\left(\frac{\widetilde{L}_{ij}}{b_{ij}}\right)\right) \tag{17}$$

where K_{ij} is a gain that regulates the magnitude of the potential energy, and b_{ij} will be the boundary of the saturation function of the force.

The Figure 2 shows the graphical shape of the potential interactive energy function. The interpretation of this function is the following: when the rotorcraft is not at its desired separation, it is going to exist a potential energy, and as the distance error is increasing in magnitude, the potential energy is increasing too.

The total structural potential energy from all the robots around the i^{th} robot is then

$$\mathcal{U}_i = \sum_{j \neq i} \mathcal{U}_{ij} \tag{18}$$

The corresponding structural force is the negative gradient of the structural potential energy. The force in the case of the robot i with respect to the robot j is

$$f_{ij} = -\nabla\mathcal{U}_{ij} = K_{ij}\left[b_{ij}\tanh\left(\frac{\widetilde{L}_{ij}}{b_{ij}}\right)\right]\frac{\boldsymbol{\xi}_j - \boldsymbol{\xi}_i}{L_{ij}} \tag{19}$$

From Figure 3 we notice that the potential force will be saturated, bounded by $K_{ij}b_{ij}$ and $-K_{ij}b_{ij}$. The force in robot i will be attractive if the difference $L_{ijd} - L_{ij}$ is positive, and the structural force will be negative otherwise. The bounded force is a good option to maintain bounded bounded velocities in the aircrafts.

To take the formation to its desired position, the errors have to be considered with respect to the goal. The distance is computed as follows

$$L_{ig} = \|\boldsymbol{\xi}_g - \boldsymbol{\xi}_i\| \tag{20}$$

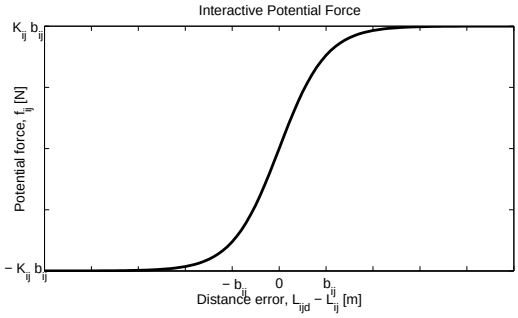

Fig. 3: Graph of the potential force function

where $\boldsymbol{\xi}_g$ is the position of the goal, and the formation distance error is represented by

$$\widetilde{L}_{ig} = L_{igd} - L_{ig} \tag{21}$$

where L_{igd} is the desired separation between the i^{th} robot and the goal position. Note: the desired separation between one rotorcraft and the goal will be selected as $L_{1gd} = 0$, and the desired separation between each other robot and the goal will be the desired separation L_{i1d}. The functions for the potential energy $\mathcal{U}_{ig}$ and the force f_{ig} are similar to (17) and (19).

Then, the total structural force acting on the i^{th} rotorcraft, is

$$F_i = -\nabla \mathcal{U}_i = \sum_{j \neq i} f_{ij} + f_{ig} \tag{22}$$

The total structural force F_i is a vector that contains a component in the x axis, denoted by F_{ix}, and a component in the y axis, denoted by F_{iy}.

The Figure 4 shows a graphical interpretation of the artificial potential force on the i^{th} rotorcraft. The x, y components of the structural force F_i are reflected on the body's frame of the i^{th} rotorcraft.

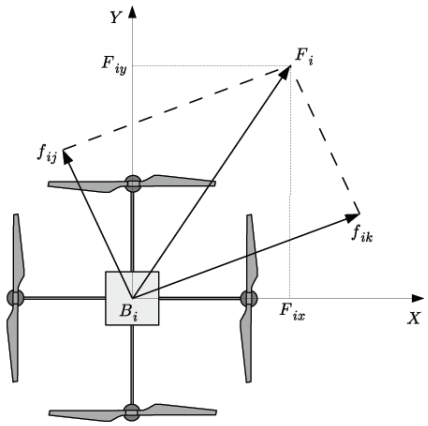

Fig. 4: Diagram of the structural force vector

III-B. Obstacle Avoidance

In order to reach obstacle avoidance, a repulsive potential energy (S. S. Ge and Y. J. Cui, 2000) has to be defined. The repulsive potential energy only acts in a region nearby the obstacle.

The function to define the repulsive potential energy is

$$\mathcal{U}_{repi} = \begin{cases} \frac{1}{2} K_{repi} \left(\frac{1}{L_{iobs}} - \frac{1}{L_0} \right)^2, & L_{iobs} \leq L_0 \\ 0, & L_{iobs} > L_0 \end{cases} \tag{23}$$

where K_{repi} is constant, $L_{iobs} = \|\boldsymbol{\xi}_{obs} - \boldsymbol{\xi}_i\|$ is the distance between the center of mass of the helicopter and the nearest border of the obstacle, and L_0 is the distance at which the repulsive function $\mathcal{U}_{repi}$ begins to act. The corresponding repulsive force is given by

$$F_{repi} = -\nabla \mathcal{U}_{repi} \tag{24}$$

and is expressed as

$$F_{repi} = \begin{cases} K_{repi} \left(\frac{1}{L_{iobs}} - \frac{1}{L_0} \right) \frac{\boldsymbol{\xi}_{obs} - \boldsymbol{\xi}_i}{L_{iobs}^3}, & L_{iobs} \leq L_0 \\ 0, & L_{iobs} > L_0 \end{cases} . \tag{25}$$

The repulsive force, thus, have to be added to the total structural force

$$F_i = \sum_{j \neq i} f_{ij} + f_{ig} + F_{repi} \tag{26}$$

III-C. Altitud and Yaw Control

The altitude and yaw control are supposed to take each rotorcraft to a desired altitude z_d and to a yaw angle $\psi = 0$ at the beginning and maintain in that desired position and angle during the rest of the time.

The vertical position control is obtained through the control input

$$u = [(k_{pz}\tilde{z} - k_{vz}\dot{z}) + mg] \frac{1}{\cos\theta \cos\phi} \tag{27}$$

with $\tilde{z} = z_d - z$ as the position error in z. k_{pz} and k_{vz} are positive constants, so u is a PD altitud control. The angles θ, ϕ should be maintained in small values to avoid singularities.

The yaw control is

$$\tau_\psi = -k_{p\psi}\psi - k_{v\psi}\dot{\psi} \tag{28}$$

where $k_{p\psi}$ and $k_{v\psi}$ denote the proportional and derivative constants for the PD yaw control.

After a finite time, $\tilde{z}$, $\dot{z}$, ψ and $\dot{\psi} \to 0$, and the system (8) - (13) is reduced to

$$\ddot{x} = g \tan\theta \tag{29}$$

$$\ddot{y} = -g \frac{\tan\phi}{\cos\theta} \tag{30}$$

$$\ddot{\theta} = \tau_\theta \tag{31}$$

$$\ddot{\phi} = \tau_\phi \tag{32}$$

III-D. Nested Saturation Control

This controller was proposed to globally asymptotically stabilize a chain of n integrators with one input (A. R. Teel, 1992), (E. N. Johnson and S. K. Kannan, 2003). We are going to present the method for the case of four integrators. Let

$$\dot{x}_1 = \alpha x_2 \quad (33)$$
$$\dot{x}_2 = \beta x_3 \quad (34)$$
$$\dot{x}_3 = \gamma x_4 \quad (35)$$
$$\dot{x}_4 = u \quad (36)$$

be a system of four integrators in cascade, where $\alpha, \beta, \gamma \neq 0$ are constants.

A control law to stabilize the system (33)-(36) is

$$u = -\sigma_{b_4}(k_4 z_4 + \sigma_{b_3}(k_3 z_3 + \sigma_{b_2}(k_2 z_2 + \sigma_{b_1}(k_1 z_1)))) \quad (37)$$

where $\sigma_{b_i}(.)$ is a saturation function of the form

$$\sigma_{b_i}(s) = \begin{cases} -b_i; & s < b_i \\ s; & |s| \leq b_i \\ b_i; & s > b_i \end{cases} \quad (38)$$

and $b_i > 0$ is constant.

The coordinate transformation is given by

$$z_4 = x_4 \quad (39)$$
$$z_3 = z_4 + \frac{k_4}{\gamma} x_3 \quad (40)$$
$$z_2 = z_3 + \frac{k_3}{\gamma} x_3 + \frac{k_3 k_4}{\beta\gamma} x_2 \quad (41)$$
$$z_1 = z_2 + \frac{k_2}{\gamma} x_3 + \frac{k_2 k_3 + k_2 k_4}{\beta\gamma} x_2 + \frac{k_2 k_3 k_4}{\alpha\beta\gamma} x_1 \quad (42)$$

Choosing appropriate values for the boundaries b_i and the gains k_i, the system is stable.

III-E. Position Control

The nested saturation control have been successfully applied in the four-rotor rotorcraft (P. Castillo et al., 2004), (P. Castillo et al., 2005a), (P. Castillo et al., 2005b), (A. Sanchez et al., 2008). However, this control law never had been applied in a cooperative task. In this subsection we set out the way to link the formation computed force with the rotorcrafts position control. The potential force is responsible to generate the path to direct each rotorcraft to its desired position, avoiding collisions, meanwhile the nested saturation control is responsible to execute the movement of each aircraft.

Pitch Control (θ, x)

Let consider the system given by the Equations (29) and (31). If we impose a very small upper bound on $|\theta|$ in such way that the difference $\tan(\theta) - \theta$ is arbitrarily small. Therefore, the subsystem to the i^{th} rotorcraft is reduced to

$$\ddot{x}_i = g\theta_i \quad (43)$$
$$\ddot{\theta}_i = \tau_{\theta i} \quad (44)$$

which represents a system of four integrators in cascade. Drawing an analogy between the system (43)-(44) and the system (33)-(36), we have that $x_1 = \tilde{x}_i = x_{id} - x_i$, $x_2 = \dot{x}_i$, $x_3 = \theta_i$, $x_4 = \dot{\theta}_i$ and $\alpha = -1$, $\beta = g$, $\gamma = 1$. Thus, for the i^{th} rotorcraft, the diffeomorphism is

$$z_{4i} = \dot{\theta}_i \quad (45)$$
$$z_{3i} = z_{4i} + k_{4i}\theta_i \quad (46)$$
$$z_{2i} = z_{3i} + k_{3i}\theta_i + \frac{k_{3i}k_{4i}}{g}\dot{x}_i \quad (47)$$
$$z_{1i} = z_{2i} + k_{2i}\theta_i + \frac{k_{2i}(k_{3i}+k_{4i})}{g}\dot{x}_i - \frac{k_{2i}k_{3i}k_{4i}}{g}\tilde{x}_i \quad (48)$$

According to (37), the pitch control is

$$\tau_{\theta i} = -\sigma_{b_{4i}}(z_{4i} + \sigma_{b_{3i}}(z_{3i} + \sigma_{b_{2i}}(z_{2i} + \sigma_{b_{1i}}(z_{1i})))) \quad (49)$$

It is well-known that this control asymptotically stabilizes one rotorcraft, taking it to a desired position x_{id}. The way to link the force computed, which depends on the position errors, with the control law that stabilizes each rotorcraft, is choosing $x_{id} = x_i + F_{xi}$. Thus

$$z_{1i} = z_{2i} + k_{2i}\theta_i + \frac{k_{2i}k_{3i} + k_{2i}k_{4i}}{g}\dot{x}_i - \frac{k_{2i}k_{3i}k_{4i}}{g}F_{ix} \quad (50)$$

each state converges to zero, when $z_{4i} \to 0$, $\dot{\theta}_i \to 0$, in the same way, when $z_{3i} \to 0$, $\theta_i \to 0$, when $z_{2i} \to 0$, $\dot{x}_i \to 0$, and $z_{1i} \to 0$ just after $F_{ix} \to 0$, and it happens when the state x_i has reached its desired position in the formation.

Roll Control (ϕ, y)

Let consider the system given by the Equations (30) and (32). If we impose a very small upper bound on $|\phi|$ in such way that the difference $\tan(\phi) - \phi$ is arbitrarily small; also we have considered before that θ was going to be maintained small in such way that $\cos\theta \approx 1$. Therefore, the roll subsystem to the i^{th} rotorcraft is reduced to

$$\ddot{y} = -g\phi \quad (51)$$
$$\ddot{\phi} = \widetilde{\tau}_{\phi} \quad (52)$$

Drawing an analogy between the system (43)-(44) and the system (33)-(36), we have that $x_1 = \tilde{y}_i = F_{iy}$, $x_2 = \dot{y}_i$, $x_3 = \phi_i$, $x_4 = \dot{\phi}_i$ and $\alpha = -1$, $\beta = -g$, $\gamma = 1$. Thus, for the i^{th} rotorcraft is

$$z_{4i} = \dot{\phi}_i \quad (53)$$
$$z_{3i} = z_{4i} + k_{4i}\phi_i \quad (54)$$
$$z_{2i} = z_{3i} + k_{3i}\phi_i - \frac{k_{3i}k_{4i}}{g}\dot{y}_i \quad (55)$$
$$z_{1i} = z_{2i} + k_{2i}\phi_i - \frac{k_{2i}(k_{3i}+k_{4i})}{g}\dot{y}_i + \frac{k_{2i}k_{3i}k_{4i}}{g}F_{iy} \quad (56)$$

According to (37), the pitch control is

$$\tau_{\phi i} = -\sigma_{b_{4i}}(z_{4i} + \sigma_{b_{3i}}(z_{3i} + \sigma_{b_{2i}}(z_{2i} + \sigma_{b_{1i}}(z_{1i})))) \quad (57)$$

Given that the nested saturation controller takes each rotorcraft to its desired position asymptotically, the entire formation is asymptotically stable.

IV. SIMULATION RESULTS

TABLE I: Parameter and constant values

Type	Parameter	Value
Rotorcraft model	m	1 Kg
	g	9.81 m/s^2
Potential function	K_{ij}	1.4
	b_{ij}	3
Controller constants	k_{1i}	3
	k_{2i}	0.9
	k_{3i}	0.75
	k_{4i}	0.7
Controller boundaries	b_{1i}	0.8
	b_{2i}	0.6
	b_{3i}	0.3
	b_{4i}	0.15

The simulations was realized in MATLAB Simulink ™, each rotorcraft was simulated with the same model parameters (see Table I). In this method the formation bearing is not controlled, just the distances among aircrafts, so the final formation structure could have whichever orientation. We present a simulation of three rotorcrafts trying to arrange in a Delta formation. The desired distances among rotorcrafts are expressed in the following matrix

$$L_d = [L_{ijd}] = \begin{bmatrix} 0 & 2 & 2 \\ 2 & 0 & 2 \\ 2 & 2 & 0 \end{bmatrix} \quad (58)$$

and the distance terms $L_{1gd} = 0$, $L_{2gd} = L_{21d} = 2$ and $L_{3gd} = L_{31d} = 2$. The initial positions are $\boldsymbol{\xi}_1^0 = (-1{,}7, -0{,}2)$, $\boldsymbol{\xi}_2^0 = (-2{,}8, 1{,}5)$, $\boldsymbol{\xi}_3^0 = (-2{,}5, -2{,}0)$, and the goal position is $\boldsymbol{\xi}_g = (3, 2)$. The Figure 5 shows the trajectories followed by the rotorcrafts. The sign $\times$ represents the initial position, meanwhile the final position is marked with a mini-rotorcraft.

The Figure 6 shows the distance errors $\widetilde{L}_{ij} = L_{ijd} - L_{ij}$. From the figure we can notice that until the first 15 seconds, the formation is settle down, however, the distance errors are not zero until about 67 seconds when the leader has practically reached the goal position; this behavior is due to the controller is just for regulation. The reduction of the distance errors $\widetilde{L}_{ij}$ during the movement can be achieved at the expense of the time. However, the time in which the structure achieve the goal position seems to be very long, and this is because of two reasons: the first is that the nested saturation controller works with small signals, so that the speed of each aircraft is limited to its saturating bound; the second and more significant reason is that the computed input force for each rotorcraft depends of all the rotorcrafts

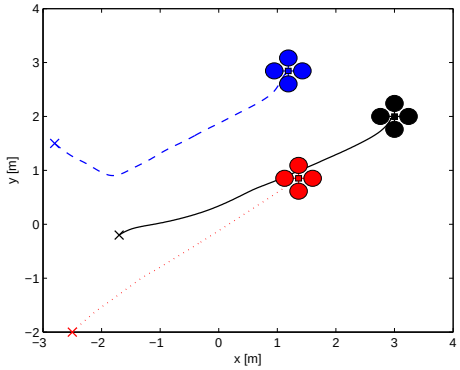

Fig. 5: Formation trajectory without presence of obstacles.

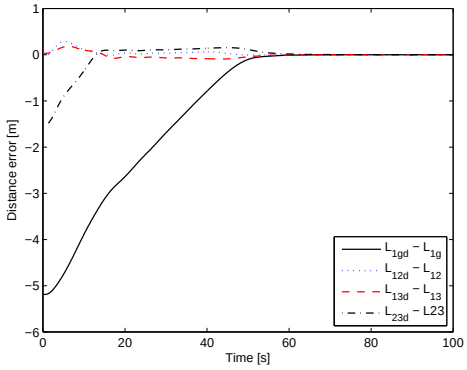

Fig. 6: Distance errors $\widetilde{L}_{ij}$.

in the structure and each rotorcraft can not go freely to its goal position, but has to pull slowly the other rotorcrafts.

Unlike other kinds of formation controllers that in presence of obstacles the structure loses temporary the formation in order to avoid that obstacles, with a controller based on potential functions, the formation tries to be maintained in every time, because if an obstacle is obstructing the trajectory of one aircraft toward the goal, all the formation is going to move to avoid the obstacle.

In the Figure 7 the trajectories of the aircrafts in presence of one obstacle are shown. The obstacle obstructs the trajectory of the leader and one of the followers, comparing the trajectory in presence of an obstacle with the trajectory in Figure 6, it is not difficult to notice a change in the formation path, and also in the orientation of the total structure. The distance errors $\widetilde{L}_{ij}$ are shown in Figure 8.

The figure 9 shows the control signals of pitch (τ_θ) and roll (τ_ϕ) for the first rotorcraft. The control signals are in a saturated region just at the beginning, τ_θ is bounded in 0.3 and τ_ϕ in -0.15, and after that moment of saturation, they remain in small values and tend to 0.

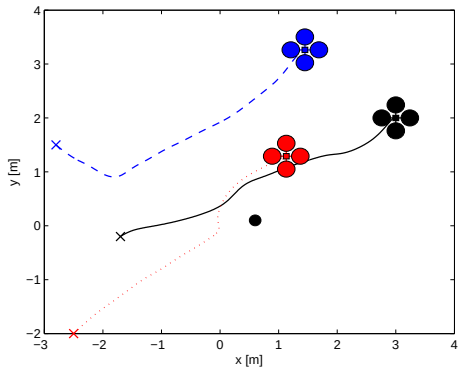

Fig. 7: Formation trajectory in presence of one obstacle.

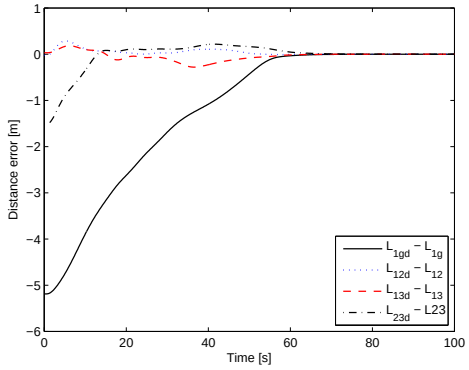

Fig. 8: Distance errors $\widetilde{L}_{ij}$.

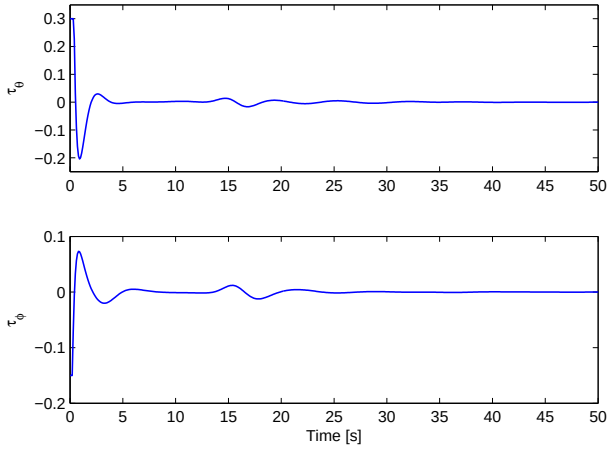

Fig. 9: Control signals in the first rotorcraft.

V. CONCLUSIONS

The formation control for mobile robots have been widely studied, despite that, it is hard to find works related with helicopter's formations. The potential artificial functions represent an effective way to reach formations among vehicles. It consists in generate artificial functions that attract or repulse the rotorcrafts to the point of minimal potential energy. The potential energy acts through a potential force that leads each rotorcraft to any position to construct the formation. In this paper we have proposed the way to link the computed potential force with a quad-rotor controller based on nested saturation. Also, the obstacle avoidance is dealt with satisfactory simulation results.

REFERENCES

P. Castillo, A. Dzul and R. Lozano (2004). "Real-time stabilization and tracking of a four-rotor mini rotorcraft", *IEEE Transactions on Control Systems Technology*, Vol. 12, No. 4, pp 510-516, July.

P. Castillo, R. Lozano and A. Dzul (2005a). "Modelling and control of mini-flying machines", *Ed. Springer-Verlag*, ISBN: 1-85233-957-8.

P. Castillo, R. Lozano and A. Dzul (2005b). "Stabilization of a mini rotorcraft having four rotors", *IEEE Control Systems Magazine*, Vol. 25, No. 6, pp 45-55, December.

Travis Dierks and S. Jagannathan (2009). "Neural Network Control of Mobile Robot Formations Using RISE Feedback", *IEEE Transactions on Systems, Man, and Cybernetics*, Part B: Cybernetics, Vol. 39, No. 2, April.

Farbod Fahimi (2008). "Full formation control for autonomous helicopter groups", *Robotica*, Volume 26 , Issue 2, Pages 143-156.

S. S. Ge and Y. J. Cui (2000). "New Potential Functions for Mobile Robot Path Planning", *IEEE Transactions on Robotics and Automation*, Vol. 16, No. 5, October.

E. N. Johnson and S. K. Kannan (2003). "Nested Saturation with Guaranteed Real Poles", *Proceedings of the American Control Conference*. Denver, Colorado, pp. 497-502, June 4-6.

Yi Liang and Ho-Hoon Lee (2006). "Decentralized formation control and obstacle avoidance for multiple robots with nonholonomic constraint", *Proceedings of the 2006 American Control Conference*, Mineapolis, Minnesota, USA, June 14-16, 2006.

Tobias Paul, Thomas R. Krogstad and Jan Tommy Gravdahl (2008). "Modelling of UAV formation flight using 3D potential field", *Simulation Modelling Practice and Theory*, Volume 16, Issue 9, October, Pages 1453-1462.

M. Saffarian and F. Fahimi (2007). "A Control Framework for Configurable Formation Flight of Autonomous Helicopters", *45th AIAA Aerospace Sciences Meeting and Exhibit*, 8 - 11 January, Reno, Nevada.

M. Saffarian and F. Fahimi (2008). "Control of helicopters formation using non-iterative Nonlinear Model Predictive approach", *American Control Conference*, 11-13 June, Page(s): 3707 - 3712.

A. Sánchez, P. Garcia, P. Castillo and R. Lozano (2008). "Simple Real-time Stabilization of a VTOL aircraft with Bounded Signals", *AIAA Journal of Guidance*, Control and Dynamics, Vol. 31, No. 4, pp. 1166-1176. ISSN 0731-5090.

A. R. Teel (1992) "Global stabilization and restricted tracking for multiple integrators with bounded controls", *Systems and Control Letters*.